ELSEVIER

Journal of Luminescence 98 (2002) 355–365

JOURNAL OF LUMINESCENCE

www.elsevier.com/locate/jlumin

High bandwidth spectral gratings programmed with linear frequency chirps

R. Reibel*, Z. Barber, M. Tian, W.R. Babbitt

Department of Physics, Montana State University, Bozeman, MT, 59717, USA

Abstract

Temporally overlapped linear frequency chirps (TOLFCs), a novel method for programming a spatial-spectral grating, are used to demonstrate grating bandwidths in excess of 2 GHz. The proper operating conditions for this method are discussed along with grating efficiency measurements. A Maxwell–Bloch simulator, which incorporates arbitrary phase functions, is used to simulate this programming method and to investigate the grating dynamics of accumulated programming using TOLFCs.

PACS: 42.50.md; 42.50.Gy; 42.50.Ct

Keywords: Linear frequency chirp; Spatial-spectral holography; True time delay; Stimulated photon echo

1. Introduction

Stimulated photon echoes (SPE) or spatial-spectral holography (SSH) can be utilized for several high bandwidth (>1 GHz) applications, such as true time delay (TTD) steering of phased array radar and communication systems. SSH has been effectively demonstrated for many of these applications at both low and high bandwidths [1–4]. In most previous demonstrations, expensive laser systems were required. In order to make SSH a more practical and affordable technique, less expensive, more compact, and higher efficiency systems should be employed. To achieve this goal, new methods for programming high bandwidth gratings with low power diode lasers have been explored.

Low cost, high bandwidth chirped external cavity diode lasers (CECDLs) have recently been built and characterized [5,6]. These lasers have the ability to create linear frequency chirps (LFCs) up to 40 GHz depending upon the cavity configuration. As low cost alternatives to specialized laser systems, these lasers will have a direct impact upon the future practicality of SSH. In this paper, we discuss and examine a programming technique that, in conjunction with a CECDL, will make SSH more practical for TTD, arbitrary waveform generation, and correlative systems [7]. This technique uses two temporally overlapped LFCs to program high bandwidth gratings. Simulations, using a Maxwell–Bloch simulator, which incorporates arbitrary phase functions, are utilized to examine in detail the gratings created. These simulations are used to explore issues relevant to high bandwidth LFC programming such as power scaling versus bandwidth and accumulation. We

*Corresponding author. Tel.: +1-406-994-79-88.
E-mail address: reibel@physics.montana.edu (R. Reibel).

0022-2313/02/$ - see front matter
PII: S0022-2313(02)00290-9

also experimentally demonstrate the production of high bandwidth spatial-spectral gratings using a CECDL for TTD applications.

The paper is divided into three main sections. First, a discussion and overview of programming with TOLFCs is given. Second, the results of both low and high bandwidth experiments are presented which use TOLFCs. Finally, the Maxwell–Bloch simulator is discussed and numerical results compared to experiment.

2. Theory and discussion

2.1. Temporally overlapped linear frequency chirped programming

In order to create a TTD using spatial spectral holography, a spectral grating must be stored or programmed into the SSH medium. This was typically done using two brief pulses separated by a time delay, τ_{21}. The two pulses interfere to produce a spectral grating of period $1/\tau_{21}$ within the inhomogeneously broadened absorber (IBA). This spectral grating can be probed some time, t_p, later using a third pulse (here $t_p \gg T_2$). The third pulse is diffracted by the spectral grating and creates a time-delayed replica of itself known as a stimulated photon echo. The probe pulse need not be of the same temporal shape as the first two pulses, which created the grating. In fact, it is highly desired that the probe pulse carry high bandwidth signals, which must be time delayed for some application such as the steering of phased array radar. In order for these high bandwidth signals to be diffracted and produce an SPE, the grating itself must be of greater bandwidth than the signal. In the case of programming a grating with brief pulses, this requires that the brief pulses' temporal duration be extremely short to cover a large bandwidth. For the case of Tm^{3+}:YAG, the inhomogeneous broadening is on the order of 20 GHz. To utilize the entire bandwidth of the material requires brief pulses on the order of tens of picoseconds. However, using brief pulses to program large bandwidths requires large peak powers which can lead to crystal damage or the need to accumulate many lower power brief pulses [8].

LFC programming of optical coherent transient (OCT) TTD has two significant advantages over brief pulse programming. The first is the reduction in the required laser power compared to brief pulses [9]. As stated above, brief pulse programming requires an inverse relationship for programming bandwidth and temporal duration of the pulse. Essentially, to program a large bandwidth, the brief pulse must be very short in time. However, LFCs can have relatively long temporal duration and still program large bandwidths. This allows more optical energy to be transferred to the medium compared to brief pulse programming. Thus efficient, high bandwidth gratings can be programmed with relatively low power diode laser systems. Even greater power efficiency is achieved through accumulation with repetitive programming. Accumulation, the technique of repeating programming pulses on a time scale greater than the coherence time, T_2, but less than the upper state lifetime, T_1, has been shown to be an effective way of building high bandwidth TTD gratings [8,10–11]. Thus, diode laser systems with a few tens of milliwatts of power can maintain an efficient OCT TTD grating.

The second advantage of chirped pulse programming is the ability to achieve variable time delay via frequency shifting [9]. Fig. 1(a) shows how two non-overlapped LFCs, each with the same chirp rate, γ, can be used to create a spectral grating. These LFCs, each of temporal length τ_c and bandwidth $B = \gamma\tau_c$, are separated by some time delay, denoted by τ_{21}. If the LFCs each start with the same frequency, the time delay is given simply by the temporal separation between the two LFCs, τ_{21}. However, if the start frequency of the two LFCs is different the time delay is given by

$$\tau_D = \tau_{21} + \frac{\delta}{\gamma}, \tag{1}$$

where δ represents the frequency difference between the start frequency of the first pulse minus the start frequency of the second pulse. Thus, the delay can be controlled by either the timing or the frequency offset of the two LFCs, or both. There are drawbacks to this approach for high bandwidth TTD [12]. First, efficient operation requires the duration of the LFCs, τ_c, to be less than the

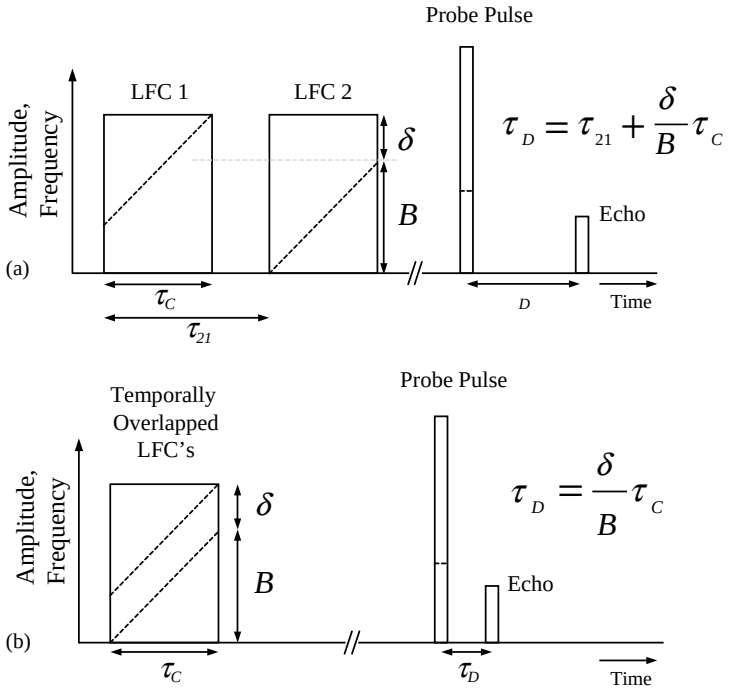

Fig. 1. This figure shows two methods that vary the programmed true time delay via frequency offsetting chirps. (a) Two LFCs separated by a delay τ_{21}. (b) Two temporally overlapped LFCs. Solid lines represent field amplitude and dashed lines represent instantaneous frequencies of LFCs and probe.

coherence time, T_2, putting high demands on chirp driver circuitry. Second, broadband flat frequency response requires $\delta \ll B$ and thus the fractional dynamic range of delay times ($\tau_{\mathrm{Dmax}}/\tau_{\mathrm{Dmin}}$) is much <1. Finally, while the LFCs could be produced sequentially by a single laser, this requires stringent constraints on the allowable phase deviation between the produced LFCs.

Recently, we improved upon this technique by removing the time delay from the two time separated LFCs allowing a single chirp to be the source of the offset LFCs [7]. The temporally overlapped LFCs (TOLFC) are shown in Fig. 1(b). In this approach, it is the frequency offset that directly controls the time delay of the output echo signal. The TOLFC technique adds significant benefits to the simplification of OCT TTD devices. Broadband TTD control is reduced simply to frequency shifts that are made with narrow band devices, such as acousto-optic modulators (AOMs). The fractional dynamic range of delay times is much >1, and thus time delays can range from close to 0 to approximately T_2. Also, the chirp duration, τ_c can greatly exceed T_2, enabling efficient gratings with less optical power. In addition, long chirp duration shortens the δ required for a given τ_D, allowing smaller frequency offsets to tune high bandwidth TTDs over a wide range of delays.

Practical implementation of the TOLFC technique to produce high bandwidth TTD gratings requires several issues to be addressed. First, what are the proper operating conditions of the TOLFC method for a given chirp B and τ_c. Second, for a single programming sequence, what is the upper bandwidth we can reach given a diode lasers power and the SSH materials upper state lifetime. And finally, can this bandwidth limit be pushed further by accumulation of the programming sequence. To help answer these questions, a combination of theory, simulations and experiment have been performed.

2.2. Grating efficiency versus programming bandwidth and chirp duration

LFCs are a more efficient solution for programming compared to using brief pulses. However, achieving maximum efficiency requires optimizing the chirp parameters. The efficiency of a grating, η, is defined as the ratio of the peak echo intensity, I_e, to the peak intensity of the probe, I_p. That is

$$\eta = \frac{I_e}{I_p}. \tag{2}$$

In the linear regime (without accumulation), the echo signal in the frequency domain, $E_e(\omega)$ can be found from the relation [2]

$$E_e(\omega) \propto E_1^*(\omega)E_2(\omega)E_p(\omega). \tag{3}$$

Here, $E_1(\omega)$ and $E_2(\omega)$ are the Fourier transforms of the first and second pulses of the programming sequence, respectively, and $E_p(\omega)$ is the Fourier transformed probe pulse. If the frequency chirps have a field amplitude in the time domain of E_c and $E_1^*(\omega)E_2(\omega)$ is assumed flat over B and zero outside of B, that is $|E_1(\omega)| = |E_2(\omega)| = E_0$ on the interval $2\pi B$ of the LFC, then it can be shown that the following relation holds:

$$E_0 = E_c\sqrt{\frac{\tau_c}{B}}. \tag{4}$$

Using this equation, and assuming that the intensity in a pulse is proportional to the square of the field, we find the intensity of the echo to be

$$I_e \propto E_c^4\left(\frac{\tau_c}{B}\right)^2 I_p. \tag{5}$$

And using Eq. (2) we find for the efficiency

$$\eta \propto E_c^4\left(\frac{\tau_c}{B}\right)^2. \tag{6}$$

If the grating was programmed by a series of brief programming pulses, the echo efficiency would fall as approximately $1/B^4$. But the echo efficiency with chirped pulse programming is proportional to $1/B^2$, and thus chirps offer an advantage over brief pulses. LFC programming has the added benefit of having the echo intensity proportional to τ_c^2. Thus, the longer the chirp duration, the stronger the echo will be. So if the bandwidth is increased, the drop in efficiency can be compensated for by increasing the chirp time to keep the chirp rate constant. These traits make TOLFC programming an attractive, practical solution for high bandwidth programming.

3. Experiments

To address the issues stated at the end of Section 2, several different experiments were developed. Specifically, we wanted to use the TOLFC programming method with a high bandwidth CECDL to show production of high bandwidth TTD gratings. Along with this, we wanted to explore the operating limits of the TOLFC programming method to ensure typical operation would not introduce programming errors. Finally, since accumulation will likely be used to push future bandwidths beyond a few gigahertz, we wanted to show that the TOLFC technique could accumulate efficient TTD gratings.

For a low bandwidth demonstration of the TOLFC technique, two AOMs in series were used in conjunction with an injection-locked diode laser system described elsewhere [13]. The injection locking system is capable of producing output powers after optical isolation of ~ 70 mW for these experiments. The first AOM was used to create a 40 MHz chirp and the second AOM created two LFCs offset by a frequency δ and the probe pulse. The voltage applied to the AOM was

$$V = A[\cos(2\pi(f_m - \delta/2)t) + \cos(2\pi(f_m + \delta/2)t)]. \tag{7}$$

Here f_m is the center frequency of the AOM and A is the amplitude. The light was focused tightly into this AOM keeping the angle between the two frequencies close to the diffraction limit to ensure good spatial overlap of the two frequency offset pulses. For the probe pulse $\delta = 0$, and thus the probe pulse's frequency remains centered between the offset LFCs. The programming and probe pulses and the echo were collinear in this experiment but other geometries that allow spatial isolation of the echo can be implemented. The repetition rate of the sequences was 10 Hz, which gives a time between sequences that is much

greater than the storage time of the Tm^{3+}:YAG crystal used in these experiments.

In all the experiments described here, the optical power before the crystal is approximately 30 mW. The pulse sequences are focused into a Tm^{3+}:YAG crystal cooled to 4 K with an absorption length, αL, of 1.4. The diameter at the beam waist was $\sim 35\,\mu m$. The output from the crystal was incident on a silicon photodiode with a bandwidth of 1 GHz and recorded on a digitizing oscilloscope with bandwidth of 300 MHz. T_2 of the Tm^{3+}:YAG crystal was measured by analyzing the decay of SPEs diffracted from gratings created by LFCs with $B = 20\,MHz$ for various time delays. This method gave $T_2 = 15\,\mu s$.

3.1. Operating conditions for TOLFC programming

In an ideal condition, for perfect TTD grating programming using LFCs, the spectral amplitude of the chirp would be flat over the bandwidth of the chirp. However, in reality an LFC's power spectrum includes oscillations. These oscillations in the spectral domain depend on the time bandwidth product (TBP), $B\tau_c$, of the chirp. If there is no frequency offset between a set of identical LFC programming pulses (such as in Fig. 1(a) with $\delta = 0$), each atom will see the same power and this leads to a fairly uniform spectral grating, provided the chirps have TBPs > 40. Almost no differences between TTD grating programming with brief pulses or LFCs with TBP > 40 can be detected assuming that the LFCs are identical and have no frequency offset [9]. However, in the case of TOLFC programming, the delay is entirely set by the offset frequency, δ. This can lead to the possibility that the oscillatory fluctuations of the chirp's power spectrum can play a role in grating shape. As the time delay is varied by shifting the frequency offset between the chirps, the overall grating shape can be affected by these fluctuations, leading to undesired intensity fluctuations of the echo signals. Because of the complexity of this problem, an analytic description of this process is nearly impossible. Experimentally, we have observed that for TBPs < 120 the echo intensity can be affected by these power spectrum oscillations. Fig. 2 shows echo peak intensities versus delay time for (a) TBP = 40,

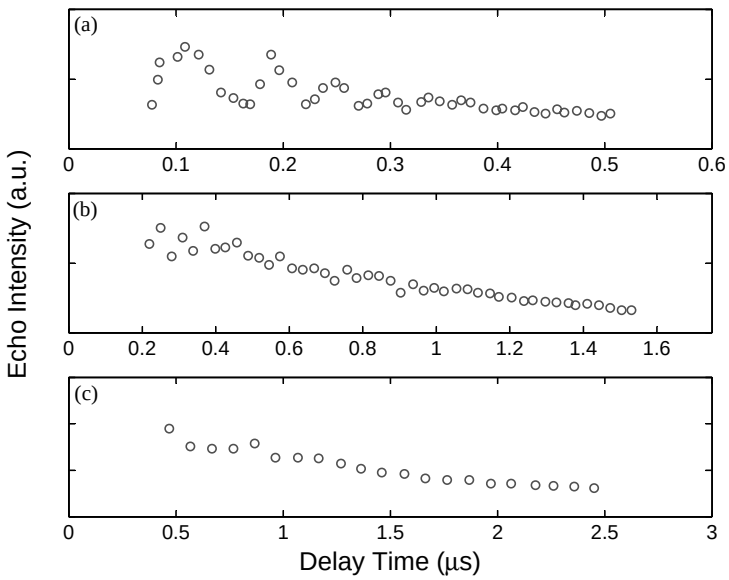

Fig. 2. Experimental echo intensities plotted versus delay time for (a) TBP = 40, (b) TBP = 120, and (c) TBP = 200. For $B\tau_c$s < 120, a periodic intensity fluctuation is observed.

(b) TBP = 120, and (c) TBP = 200. For each plot shown $B = 40\,\text{MHz}$. As can be seen from the figure, a strong periodic intensity fluctuation on the echo is seen for TBP = 40. As the TBP is increased this periodic event diminishes, as in (b) where TBP = 120, and then almost completely disappears, as in (c) where TBP = 200. Similar trends have also been observed with simulations. Thus, for practical operation, the TBP should be kept as high as possible in order to avoid such echo fluctuations. For desired high bandwidth operation, TBPs will be on the order of 10^3 and thus meet the criteria to avoid these echo fluctuations.

3.2. High bandwidth gratings

For the high bandwidth experiments, a homemade CECDL was used to create the frequency chirps [6]. The output chirps from the CECDL were amplified using the injection locking system. Output powers from the injection locking system for the high bandwidth experiments were again $\sim 70\,\text{mW}$. By using the homemade CECDL and the TOLFC programming method, we were able to create efficient TTD gratings with bandwidths from 100 MHz to beyond 2 GHz. These gratings have been probed in two different ways. First, we probed the absorption spectrum of the gratings using a $\tau_p = 100\,\mu\text{s}$ LFC with a probe bandwidth, $B_p \cong 2.4\,\text{GHz}$. Fig. 3(a) shows the transmitted probe pulse as a function of the instantaneous frequency of the probe. The programming LFC had bandwidth $B \cong 2.0\,\text{GHz}$, and $\tau_c = 30\,\mu\text{s}$ giving $\gamma \cong 68\,\text{MHz}^2$ and $\delta = 15\,\text{MHz}$. Fig. 3(b) shows an enlarged portion of (a). Here the periodicity in frequency corresponds to $\sim 4.5\,\text{MHz}$. When this plot is Fourier transformed, a frequency component is found at $0.22\,\mu\text{s}$, which matches the expected TTD of $\tau_D = \delta/\gamma = 0.22\,\mu\text{s}$.

The second method of probing these gratings is using a low bandwidth ($\sim 20\,\text{MHz}$) Fourier transform limited pulse and observing the echo pulse as the carrier frequency of this probe pulse was changed over the bandwidth of the programming chirps. This measurement ensured that the entire bandwidth was being programmed. We also used this method to verify Eq. (6). Fig. 4 shows peak intensity of the echo pulse as a function of the

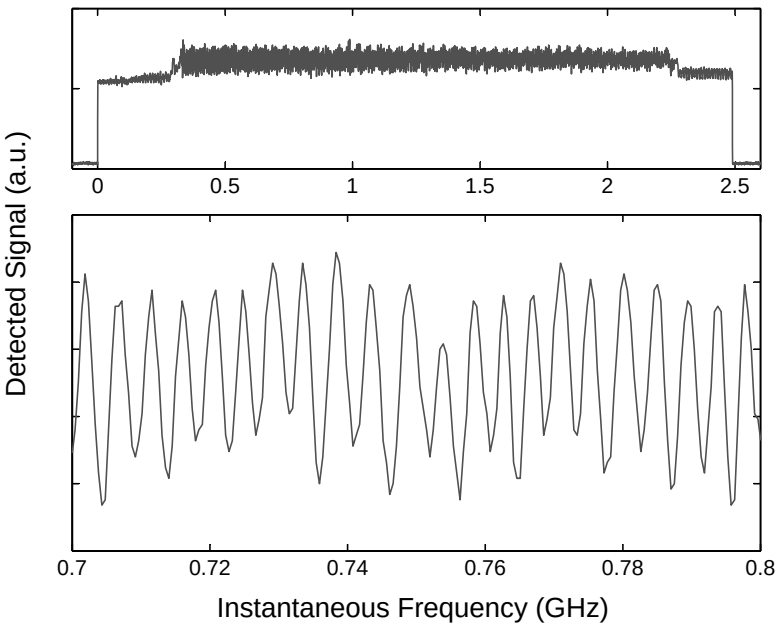

Fig. 3. (a) This figure shows the transmission of a low intensity 2.4 GHz LFC probing a 2.0 GHz TTD grating programmed with the TOLFC method. The large oscillation on the transmission is a frequency oscillation corresponding to a grating period $1/\tau_D$ where $\tau_D = 0.22\,\mu\text{s}$. (b) Shows these oscillations in greater detail.

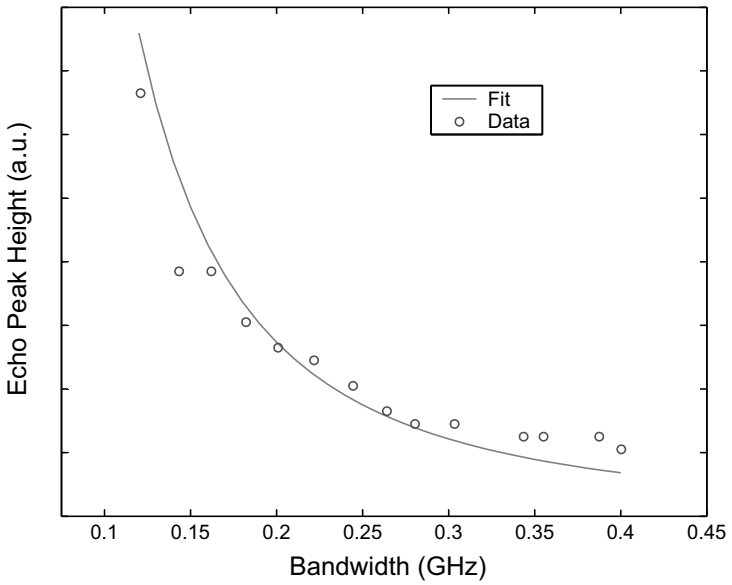

Fig. 4. This figure examines the experimental echo peak heights as a function of grating bandwidth created with the CECDL laser system. Here the programming power and τ_c are kept constant, $\tau_c = 4\,\mu s$ and the offset frequency is kept at $\delta = 20\,MHz$. The solid line is a fit using a functional dependence of $1/B^2$ according to Eq. (6).

LFC's bandwidth for $\tau_c = 4\,\mu s$ and $\delta = 20\,MHz$. The delay times are shorter than $0.6\,\mu s$ and thus T_2 effects can be ignored. The solid line is a fit using a functional dependence of $1/B^2$. As can be seen, the echo intensity decreases as predicted with $1/B^2$ dependence.

3.3. Accumulation

As discussed in the Introduction, accumulation is a way to strengthen a spectral grating using weak programming pulses. To demonstrate accumulation, a laser with frequency stability $< 1/\tau_D$ over the material lifetime ($\sim 10\,ms$) is needed. A Ti:Sapphire laser was used in conjunction with the two AOMs as described above. The Ti:Sapphire laser is locked to a regenerative spectral hole as described in Ref. [10] and has frequency stability of roughly 10 kHz. This stability allows the dynamics of accumulative programming to be studied.

The programming pulses are characterized by an individual LFC's Rabi frequency, which were $\Omega = 0.5$, 0.6, 0.9, 1.3, 1.7, and 2.2 MRad/s for this experiment chosen to show the dynamics of the accumulated gratings. These Rabi frequencies were determined from nutation experiments with non-chirped pulses [14]. Because our crystals were optically thick, the theory predicted an increase in the Ωs by approximately 20% compared to the optically thin case. We repeated programming TOLFCs with a repetition time, τ_r, of 31 μs, for N times, where $N = 1$–900. After the N programming sequences, the grating was probed using a 50 ns brief pulse. Fig. 5 details the echo intensity as a function of N for the set of programming pulses. For this figure, $\tau_c = 1\,\mu s$, $B = 40\,MHz$ and $\delta = 10\,MHz$ giving an expected delay time for the echo of $\tau_D = 250\,ns$. Because of the population dynamics, the larger programming strengths, $\Omega > 1.3$ MRad/s, are too strong and saturate the medium leading to inefficient gratings. The weaker programming strengths, $\Omega < 0.6$ MRad/s, are not strong enough and do not accumulate an efficient grating. Between these two regimes the best accumulation can be found such as the $\Omega = 0.9$ MRad/s programming strength. These experimental results are discussed more thoroughly in Ref. [7], and are shown here for comparison with simulation.

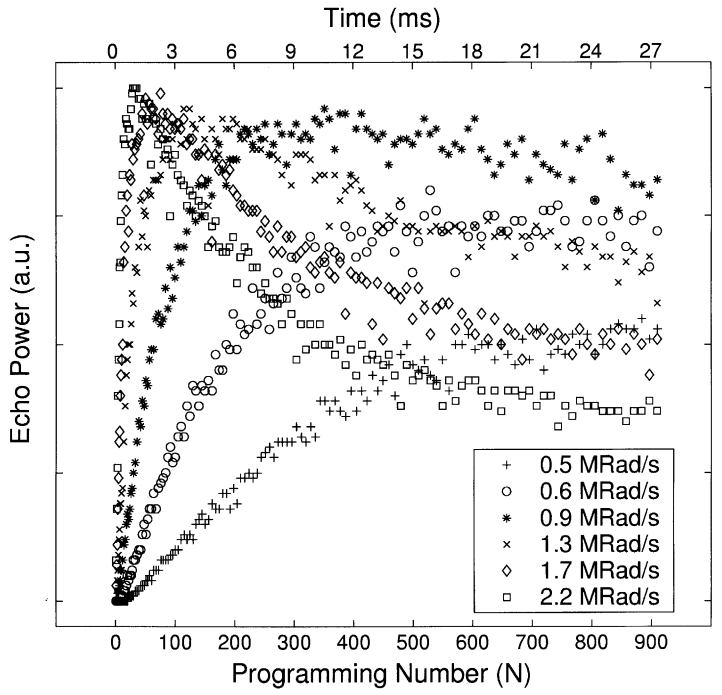

Fig. 5. This series of plots shows echo intensities vs. programming number (lower axis) or time (upper axis) measured with a frequency stabilized Ti:Sapphire laser system. The different plots are various programming strengths (Rabi frequency, Ω) as shown in the legend. Here $\tau_c = 1\,\mu s$, $\tau_D = 250\,ns$, and $\tau_r = 31\,\mu s$.

4. Simulation and analysis

In order to study the echoes shown in the previous experiments, a simulator needed to be developed that could handle chirped pulses. Traditional Bloch simulators have been used to simulate chirped pulses, but because the Beer's length of our crystal was fairly large, $\alpha L = 1.4$, propagation effects had to be included. Maxwell–Bloch simulators have previously been developed and used to study propagation effects on echoes, which showed that propagation effects have a strong impact on echo shape and intensity and can be utilized to improve signal fidelity and efficiency [15,16]. However, these simulators do not allow arbitrary phase and frequency shifts. Thus, a new simulator needed to be developed that could handle these situations in order to properly simulate LFCs. To include arbitrary phase or frequency, we write the electric field as

$$E(z,t) = \frac{\hbar}{\mu_{12}}\Omega(z,t)\cos(\omega_o t - k_z z + \phi(z,t)), \tag{8}$$

where we have assumed that the light only propagates in the positive z direction. Here, $\Omega(z,t)$ is a slowly varying amplitude function dependent upon propagation direction, z, and time, t, μ_{12} is the dipole moment, ω_o is the optical frequency, k_z is the k-vector along z, and $\phi(z,t)$ is an arbitrary phase function which is dependent upon z and t. In this form, the Bloch vector, $\vec{r}$, equation of motion in the rotating frame becomes

$$\begin{aligned}\dot{r}_1 &= -\Delta r_2 - \Omega r_3 \sin\phi,\\ \dot{r}_2 &= \Delta r_1 + \Omega r_3 \cos\phi,\\ \dot{r}_3 &= \Omega r_1 \sin\phi - \Omega r_2 \cos\phi.\end{aligned} \tag{9}$$

Here, $\Delta = \omega_a - \omega_o$ is the detuning with ω_a as the frequency of an individual atom within the inhomogeneously broadened transition. Now by

taking the Maxwell equations into account and making a transform of variables into a frame moving at the speed of the laser pulse [17], we find two separate equations for $\Omega(z,t)$ and $\phi(z,t)$ that we can integrate to find the propagation effects along the z direction

$$\frac{\partial\Omega}{\partial z} = \frac{\alpha}{2\pi}\int (r_2\cos\phi - r_1\sin\phi)g(\Delta)\,\mathrm{d}\Delta, \tag{10}$$

$$\frac{\partial\phi}{\partial z} = -\frac{1}{\Omega}\frac{\alpha}{2\pi}\int (r_1\cos\phi + r_2\sin\phi)g(\Delta)\,\mathrm{d}\Delta. \tag{11}$$

As we wanted to numerically integrate these equations, the above equation for ϕ has the difficulty of being inversely proportional to Ω. This can introduce numerical complexities when $\Omega = 0$, which can be easily avoided by keeping track of the in-phase and in-quadrature parts of the field. By defining

$$\Omega_c(z,t) = \Omega(z,t)\cos\phi,$$
$$\Omega_s(z,t) = \Omega(z,t)\sin\phi, \tag{12}$$

we can simplify the Bloch equations to

$$\dot{r}_1 = -\Delta r_2 - \Omega_s r_3,$$
$$\dot{r}_2 = \Delta r_1 + \Omega_c r_3,$$
$$\dot{r}_3 = \Omega_s r_1 - \Omega_c r_2$$

and the propagation equations then become

$$\frac{\partial\Omega_c}{\partial z} = \frac{\alpha}{2\pi}\int r_2 g(\Delta)\,\mathrm{d}\Delta, \tag{13}$$

$$\frac{\partial\Omega_s}{\partial z} = -\frac{\alpha}{2\pi}\int r_1 g(\Delta)\,\mathrm{d}\Delta. \tag{14}$$

These equations are numerically integrated to give the Bloch vector $\vec{r}(z,t,\Delta)$ for all z, time and detunings. We also get $\Omega_c(z,t)$ and $\Omega_s(z,t)$ for all z and time. We can find the square of the field, Ω^2, which is proportional to the observed intensity, by using

$$\Omega(z,t)^2 = \Omega_c(z,t)^2 + \Omega_s(z,t)^2. \tag{15}$$

Now we can introduce the phase function $\phi(z,t) = \pi\gamma t^2$ to simulate a linear frequency chirp. Simulations were performed using these equations and the results were used to verify the experimental situations described above.

4.1. Single programming sequence simulations

We simulated the efficiency of the grating as a function of bandwidth for two different situations. The first situation, keeps τ_c constant while varying B. A series of 100 simulations were done with programming Bs from 20 to 60 MHz in steps of 0.4 MHz. The probe pulse had a bandwidth of 10 MHz. Here, δs varied to keep the time delay constant at 0.8 μs. In Fig. 6, the circles are the simulated echo efficiencies versus the programming bandwidth. As can be seen, the echo intensity decreases as a function of the bandwidth as expected. The $1/B^2$ analytic solution is also plotted as the solid line. The dashed line is representative of the brief pulse programming method dropping off as $1/B^4$. The second situation is when the ratio τ_c/B is kept constant. In this case, there should be roughly no change in echo efficiency. As can be seen from the triangles in Fig. 6, the simulated echo efficiencies for this situation remain relatively constant. This set of simulations was done with Bs from 20 to 60 MHz in steps of 0.4 MHz, τ_cs ran from 2 to 6 μs in steps of 0.04 μs, and $\delta = 8$ MHz giving a constant $\tau_D = 0.8$ μs. The small fluctuations can be attributed to the fact that the simulations were run at low TBPs (TBP = 40–360).

4.2. Accumulation simulations

Simulation of accumulation sequences requires that the population dynamics between shots be taken into account. Since Tm^{3+}:YAG is a three level system, the accumulation simulations must include the decay rates from each of these levels. Since there are no pulses between programming shots and the time between programming is longer than T_2, we can follow a simple analytic solution between programming shots [8]. In this system, the 793 nm transition is between the $^3H_6$ and $^3H_4$ levels. The atoms on the $^3H_4$ level decay either to the $^3H_6$ or the $^3F_4$ with a branching ratio, β, of 0.56 and a decay time, T_1, of 800 μs. The atoms on the $^3F_4$ level also decay to the $^3H_6$ level with a lifetime, T_3, of 10 ms. By incorporating the population dynamics of all three levels we can successfully simulate the

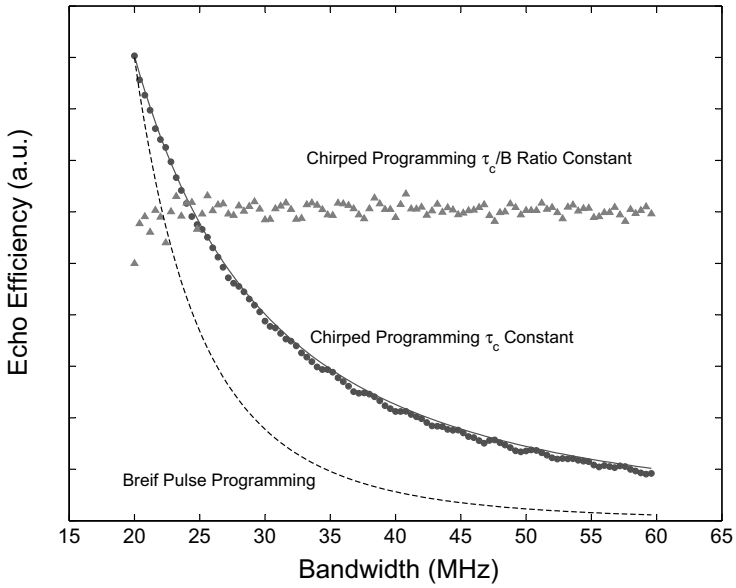

Fig. 6. Here we plot data points showing simulated peak echo height versus bandwidth for constant programming powers. Here $\tau_c = 4\,\mu s$ and δ is varied to keep τ_D constant. The solid line is calculated using the analytic functional dependence of $1/B^2$. The dashed line is a plot of the analytic dependence of a brief pulse programming versus bandwidth and is normalized for contrast. A simulated chirped programming sequence with constant τ_c/B ratio is also shown as triangles, giving relatively constant echo efficiencies. In this simulation the programming Rabi frequency was stronger to give contrast in the figure.

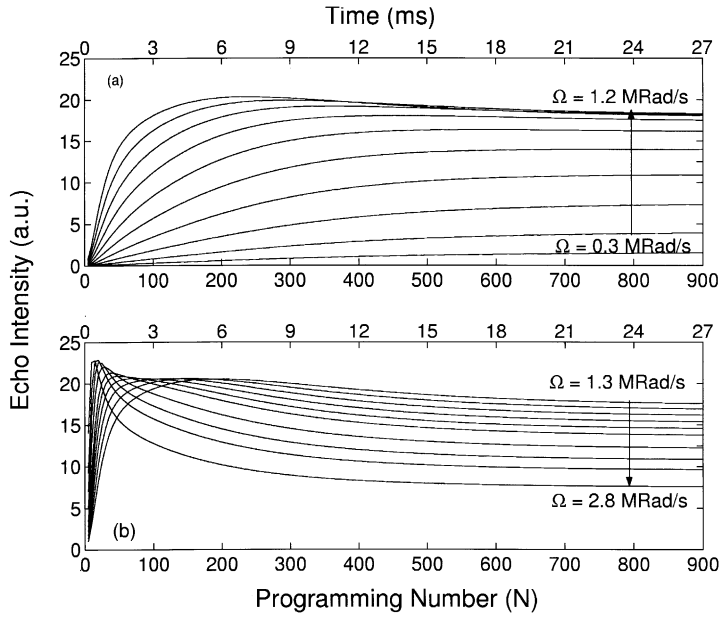

Fig. 7. Simulated accumulation sequences with $\tau_c = 1\,\mu s$, $\tau_D = 250\,ns$, and $\tau_r = 31\,\mu s$. The echo intensities are plotted versus programming number (lower axis) or time (upper axis). The different lines represent different programming strengths (Rabi frequency, Ω) with (a) showing programming Rabi frequencies from $\Omega = 0.3$ to 1.2 MRad/s in steps of 0.1 MRad/s, and (b) showing programming Rabi frequencies from $\Omega = 1.3$ to 1.8 MRad/s in steps of 0.1 MRad/s, then to 2.8 MRad/s in steps of 0.2 MRad/s.

accumulation dynamics for the TOLFCs and compare the results to the experiment.

For the accumulation simulations we set $B = 40\,\text{MHz}$, $\tau_c = 1\,\mu\text{s}$, $\tau_D = 250\,\text{ns}$, and $\tau_r = 31\,\mu\text{s}$. These values are identical to the accumulation experiments done with the frequency stabilized Ti:Sapphire laser. A series of programming Rabi frequencies was also chosen to simulate the dynamics. In Fig. 7, the results from the accumulation simulations are shown for (a) programming Rabi frequencies from $\Omega = 0.3$ to 1.2 MRad/s in steps of 0.1 MRad/s, and (b) programming Rabi frequencies from $\Omega = 1.3$ to 1.8 MRad/s in steps of 0.1 MRad/s, then from 1.8 to 2.8 MRad/s in steps of 0.2 MRad/s. The overall dynamics of the accumulation match that from the experiment. As discussed in the experimental section, the larger programming strengths, $\Omega > 1.3\,\text{MRad/s}$, are too strong and saturate the medium leading to inefficient gratings. The weaker programming strengths, $\Omega < 0.9\,\text{MRad/s}$, are not strong enough and cannot accumulate an efficient grating before the population decay sets in. For the simulations, the best accumulation can be found with Ω between 0.9 and 1.3 MRad/s. With the good agreement between simulation and experiment, we can be confident that the TOLFC accumulation method can be used in future high bandwidth studies of SSH.

5. Conclusion

We have outlined in this paper the use of the TOLFC programming method for high bandwidth programming of TTD gratings. The experimental results, backed by simulations and theory, show the expected traits of this programming method. To avoid periodic echo intensities, the TOLFC's TBP should be > 120. Along with this we showed that in the linear regime the grating efficiency as a function of the programmed bandwidth drops like $1/B^2$ (versus $1/B^4$ for brief pulse programming) and can be completely compensated for by a corresponding increase in the chirp duration. The simulations and experiments have both shown that efficient TTD gratings can be produced using the TOLFC method and that the TOLFC method will properly accumulate these gratings. These results enable the bandwidths of SSH to be pushed into the multi-gigahertz regime using affordable CECDL laser systems.

Acknowledgements

The authors would like to especially thank K.D. Merkel and Z. Cole from Spectrum Lab at MSU, for useful discussions and the generous use of equipment. We wish to gratefully acknowledge Dr. Kelvin Wagner of the University of Colorado-Boulder, Dr. William Miceli of ONR, and the Office of the Secretary of Defense DDR&E for support of this work through the MURI program grant number N00014-97-1-1006.

References

[1] T.W. Mossberg, Opt. Lett. 7 (1982) 77.
[2] X. Wang, M. Afzelius, N. Ohlsson, U. Gustafsson, S. Kroll, Opt. Lett. 25 (2000) 945.
[3] K.D. Merkel, W.R. Babbitt, Opt. Lett. 21 (1996) 1102.
[4] Y. Bai, W. Babbitt, N. Carlson, T. Mossberg, App. Phys. Lett. 45 (1984) 714.
[5] L. Ménager, L. Cabaret, I. Lorgeré, J.L.L. Gouët, Opt. Lett. 25 (2000) 1246.
[6] K. Repasky, P. Roos, L. Meng, J. Carlsten, Opt. Eng. 40 (2001) 2505.
[7] R. Reibel, Z. Barber, M. Tian, W.R. Babbitt, Opt. Lett. 27 (2002) 494.
[8] M. Tian, J. Zhao, Z. Cole, R. Reibel, W.R. Babbitt, J. Opt. Soc. Am. B 18 (2001) 673.
[9] K.D. Merkel, W.R. Babbitt, Opt. Lett. 23 (1998) 528.
[10] K.D. Merkel, R. Peters, P. Sellin, K. Repasky, W.R. Babbitt, Opt. Lett. 25 (2000) 1627.
[11] W.H. Hesselink, D.A. Wiersma, J. Chem. Phys. 75 (1981) 4192.
[12] K. Merkel, J. Zhao, K.S. Repasky, W.R. Babbitt, Proc. SPIE 3802 (1999) 246.
[13] R. Reibel, Z. Barber, M. Tian, W.R. Babbitt, Z. Cole, K.D. Merkel, J. Opt. Soc. Am. B (2001), submitted for publication.
[14] Y. Sun, G.M. Wang, R.L. Cone, R.W. Equall, W.R. Babbitt, M.J.J. Leask, Phys. Rev. B 62 (2000) 15443.
[15] C.S. Cornish, W.R. Babbitt, L. Tsang, Opt. Lett. 25 (2000) 1276.
[16] M. Azadeh, C.S. Cornish, W.R. Babbitt, L. Tsang, Phys. Rev. A 57 (1997) 4662.
[17] R. Olson, H. Lee, F. Patterson, M. Fayer, J. Chem. Phys. 76 (1982) 31.